Understanding Molecular Crystals with Dispersion-Inclusive Density Functional Theory: Pairwise Corrections and Beyond

Leeor Kronik*,[†] and Alexandre Tkatchenko*,[‡]

[†]Department of Materials and Interfaces, Weizmann Institute of Science, Rehovoth 76100, Israel
[‡]Fritz-Haber-Institut der Max-Planck-Gesellschaft, Faradayweg 4-6, 14195 Berlin, Germany

CONSPECTUS: Molecular crystals are ubiquitous in many areas of science and engineering, including biology and medicine. Until recently, our ability to understand and predict their structure and properties using density functional theory was severely limited by the lack of approximate exchange−correlation functionals able to achieve sufficient accuracy. Here we show that there are many cases where the simple, minimally empirical pairwise correction scheme of Tkatchenko and Scheffler provides a useful prediction of the structure and properties of molecular crystals.

After a brief introduction of the approach, we demonstrate its strength through some examples taken from our recent work. First, we show the accuracy of the approach using benchmark data sets of molecular complexes. Then we show its efficacy for structural determination using the hemozoin crystal, a challenging system possessing a wide range of strong and weak binding scenarios. Next, we show that it is equally useful for response properties by considering the elastic constants exhibited by the supramolecular diphenylalanine peptide solid and the infrared signature of water libration movements in brushite. Throughout, we emphasize lessons learned not only for the methodology but also for the chemistry and physics of the crystals in question. We further show that in many other scenarios where the simple pairwise correction scheme is not sufficiently accurate, one can go beyond it by employing a computationally inexpensive many-body dispersive approach that results in useful, quantitative accuracy, even in the presence of significant screening and/or multibody contributions to the dispersive energy. We explain the principles of the many-body approach and demonstrate its accuracy for benchmark data sets of small and large molecular complexes and molecular solids.
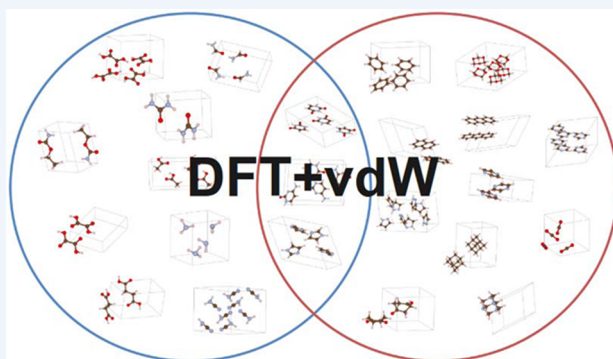
Molecular crystals are defined as crystalline solids composed of molecules bound together by relatively weak intermolecular interactions, typically consisting of van der Waals (vdW) forces and/or hydrogen bonds.[1] The molecular building blocks are often organic or metal−organic, although this is not a must. Molecular crystals play an important role in many areas of science ranging from mechanics and electronics to biology and medicine, and a large amount of effort has been dedicated to understanding their structure and properties.[1]

Molecular crystals often exhibit collective properties (i.e., properties arising from the weak intermolecular interactions) that are not found in the individual building blocks. Such properties are typically hard to predict from textbook molecular models. Therefore, first-principles calculations, based ideally on nothing more than the pertinent atomic species and the laws of quantum physics, can be of great help in elucidating such phenomena.

By far the most common first-principles electronic structure theory is density functional theory (DFT).[2−4] DFT is an approach to the many-electron problem in which the electron density, rather than the many-electron wave function, plays the central role. DFT has become the method of choice for electronic structure calculations across an unusually wide variety of fields ranging from organic chemistry[5] to condensed-matter physics[6] because it is the only currently known practical method for routinely performing fully quantum-mechanical calculations for systems with hundreds or even thousands of electrons.[7]

While DFT is exact in principle, it is always approximate in practice because relying on the electron density requires a "mapping" exchange−correlation (xc) functional that is only approximately known.[2−6] From a DFT point of view, dispersive intermolecular interactions depend on long-range correlation in the mapping xc potential.[8−10] These, however, are notoriously absent in virtually all standard approximations within DFT. As a direct result, such approximations tend to do very poorly in the description of weak interactions, greatly limiting their value for the study of molecular crystals.[11] Consequently, until recently DFT has scarcely left a footprint in this field.

In the past decade, enormous strides toward the inclusion of van der Waals interactions in DFT calculations have been made using a variety of approaches.[8,9,12,13] These can be broadly divided into several categories: (1) methods where nonlocal
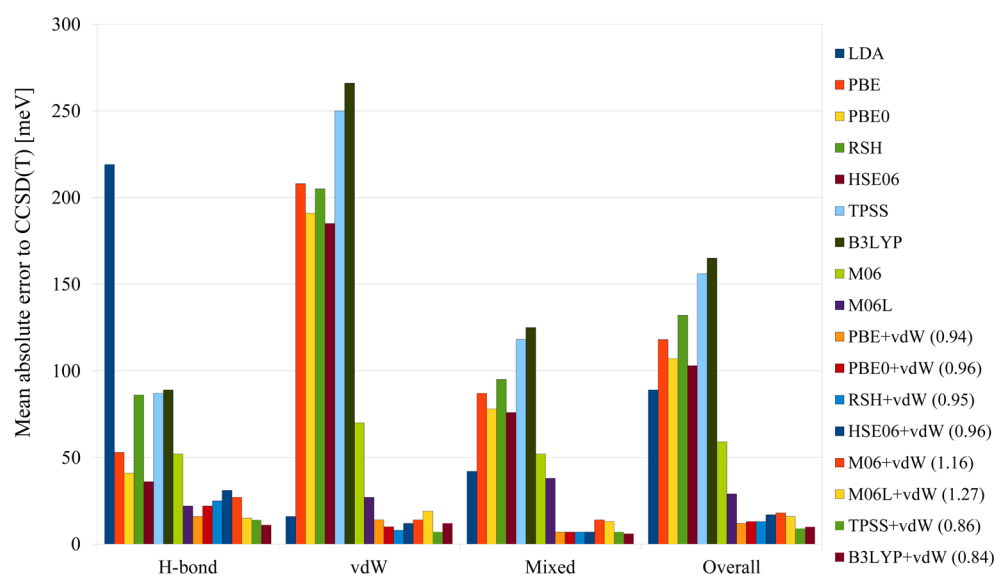
Figure 1. Mean absolute errors of different functionals with and without TS-vdW corrections with respect to CCSD(T) reference values[38] for the binding energies of the S22[34] data set. For each TS-vdW-corrected result, the optimized range parameter, s_R, is given in parentheses. Reproduced from ref 35 with additional data from ref 36. Copyright 2011, 2013 American Chemical Society.

correlation is either computed explicitly or integrated with traditional xc functionals;[10,14] (2) semiempirically parametrized xc functionals calibrated for data sets that include non-covalently interacting systems;[15−19] (3) addition of effective atom-centered nonlocal potentials;[20−22] and (4) augmentation of existing xc functionals by pairwise corrections to the internuclear energy expression that are damped at short range but provide the desired long-range asymptotic behavior.[23−28]

In the past decade, excellent work on molecular crystals, too vast to review here meaningfully, has been reported with all of the above approaches. Our literature search for molecular crystal research with DFT identified well over 150 relevant articles in the past decade but only a handful prior to that, perhaps best illustrating the vitalization of the field brought about by the new methods. Most of these studies were performed using pairwise corrections (ref 29 is one example of a thorough benchmark study). We too have chosen to devote our attention to this latter category for two main reasons. First, the computational cost associated with the evaluation of pairwise corrections is negligible, which is of great help for crystals, which may often possess large and complex unit cells. Second, the almost complete freedom in choosing the underlying xc functional is highly advantageous for obtaining an accurate description of the electronic structure.[30]

In particular, we have focused our research efforts on the Tkatchenko−Scheffler pairwise correction scheme (TS-vdW).[27] In this approach, vdW parameters (polarizability and vdW radii) are themselves functionals of the electron density, and thus the approach is only minimally empirical. Furthermore, the first-principles nature of the scheme makes it a natural starting point for more advanced treatments that go beyond it—an issue discussed in detail below.

Our (joint and separate) research efforts have focused on two central questions: (1) Can the TS-vdW scheme quantitatively describe properties of molecular crystals that are derived from total energy calculations? If so, what novel conclusions may we draw about their properties? (2) In cases where the TS-vdW scheme is insufficient, can we go beyond the pairwise picture to restore quantitative accuracy? If so, how?

And what does that teach us about the physics and chemistry of molecular crystals? In this article, we provide a concise overview of some of the answers we have found.

In pairwise correction schemes, the total energy coming from a standard DFT calculation is augmented by a dispersion-correction energy, E_{disp}, that is added to the internuclear energy term. Pairwise correction terms derived from second-order perturbation theory[31] are generally of the form:

$$E_{disp} = -\frac{1}{2} \sum_{i \neq j} f_{damp}(R_{ij}, R_{ij}^0) C_{6ij} R_{ij}^{-6}$$

(1)

where C_{6ij} is the dispersion coefficient, R_{ij} is the interatomic distance, R_{ij}^0 is the sum of the equilibrium vdW radii for the ij pair of atoms, and f_{damp} is a damping function. In the TS-vdW scheme,[27] f_{damp} is chosen to be a Fermi−Dirac function:

$$f_{damp}(R_{ij}, R_{ij}^0) = \left\{ 1 + \exp\left[-d\left(\frac{R_{ij}}{s_R R_{ij}^0} - 1 \right) \right] \right\}^{-1}$$

(2)

where d determines the "steepness" of the damping and s_R determines its range. The larger s_R is, the larger is the range of interaction for which dispersion is already well-handled by the underlying xc functional. Importantly, in TS-vdW the parameters C_{6ij} and R_{ij}^0 are not fixed but rather are themselves functionals of the electron density, $n(\mathbf{r})$. Briefly, the scheme uses accurate ab initio-computed reference values for free-atom static dipole polarizabilities and C_6 coefficients, a combination rule for deriving heteronuclear C_6 coefficients from homo-nuclear static dipole polarizabilities, and Hirshfeld partition-ing[32,33] of the DFT electron density to renormalize the vdW radii and the C_6 coefficients of an atom pair inside a molecule. The range parameter s_R is the only parameter determined empirically, by fitting it once and for all for each underlying functional using the S22 benchmark data set of weak interactions.[34]

In view of the small binding energies involved, is the resulting scheme sufficiently accurate? Figure 1[35,36] summarizes graphi-cally the performance of many xc functionals for the S22 set
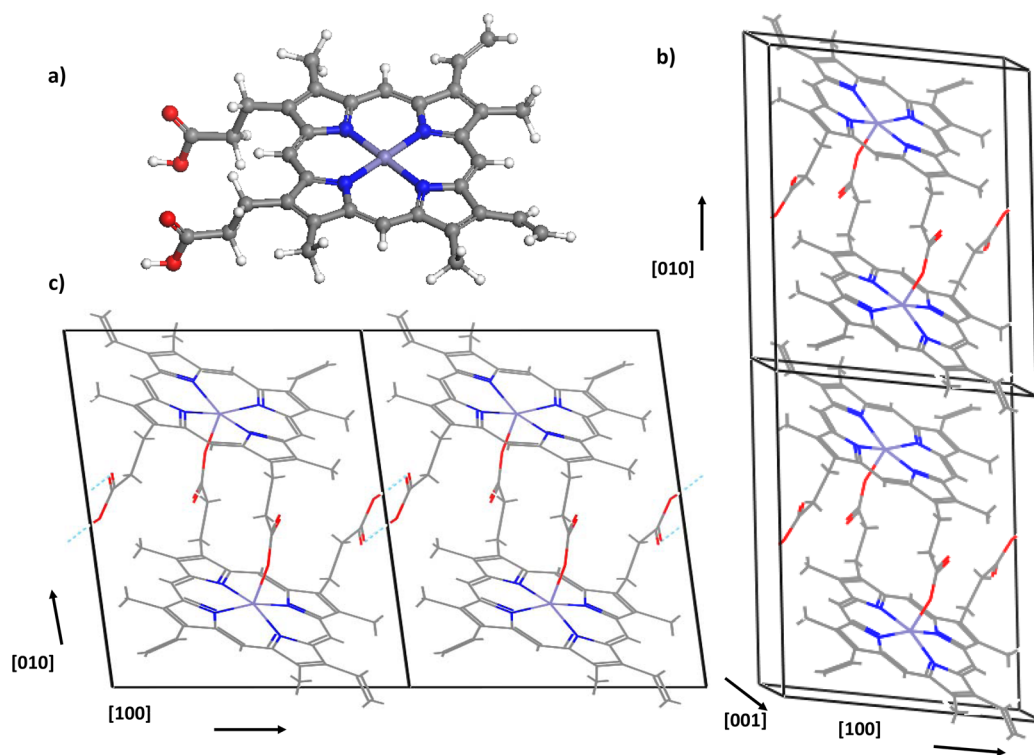
Figure 2. Schematic structural illustration of synthetic hemozoin (only the unit cell of the major phase is shown). (a) The heme monomer. (b) Stacking of heme dimers along the [010] direction. (c) Hydrogen bonds between free propionic acid groups along the [10$\bar{1}$] direction, shown as light-blue dashed lines . C atoms are shown in gray, N in blue, O in red, Fe in violet, and H in white. Some hydrogen atoms have been omitted for clarity. Reproduced from ref 41. Copyright 2011 American Chemical Society.

with and without TS-vdW corrections. Clearly, the pairwise corrections offer a significant increase in accuracy, even when applied to functionals designed to produce improved accuracy for weakly bonded systems, such as the M06 semiempirical family of functionals.[16] Furthermore, s_R is indeed found to be larger the more the underlying functional already partially accounts for midrange dispersive interactions. Therefore, double counting is avoided, and the corrected performance is satisfactory and only weakly dependent on the parent functional. The mean absolute error ranges from ~10 to ~20 meV (i.e., better than 0.5 kcal/mol) and lies within the range typically defined as "chemical accuracy". Importantly, similar performance is obtained for the larger and more varied S66 benchmark set[37] without further optimization of parameters.[35,36]

While this success is encouraging, it does not guarantee adequate accuracy for molecular crystals. Are pairwise corrections enough even in the solid-state environment? Also, when considering the structure of molecular crystals, we minimize the forces (i.e., the derivatives of the total energy with respect to atomic positions). Are the derivatives accurate enough too? Applications of the TS-vdW method to a variety of weakly bound solids (e.g., see refs 39 and 40) suggest that the answer to these questions is yes. A challenging and important system with which one can highlight this is the hemozoin crystal.[41] This crystal is biologically relevant. During the course of malaria, the parasite enters the red blood cell, where it feeds on hemoglobin, releasing the heme as a byproduct. The parasite avoids the toxicity of heme by promoting its crystallization into nonreactive hemozoin. Therefore, understanding the mechanism of hemozoin crystallization and its inhibition is important in the battle against malaria.[42]

The major phase of synthetic hemozoin is depicted in Figure 2. The repeat unit is a centrosymmetric heme cyclic dimer, where the two molecules are linked through iron–carboxylate bonds between the propionate side chain of one molecule and the central Fe atom of the other. The free propionic acid groups of the cyclic dimers form hydrogen bonds along the [10$\bar{1}$] direction. Along the [010] direction, the dimers are π-stacked. Additional stabilization is gained from dispersion interactions between the methyl and vinyl side chains of adjacent dimers. This complex interplay of organic and metal–organic bonding, hydrogen bonds, and different van der Waals interactions places stringent demands for relatively uniform accuracy across all types of bonding.

The equilibrium lattice parameters obtained with TS-vdW dispersive corrections applied to the Perdew–Burke–Ernzerhof (PBE)[43] xc functional were found to be very close to the experimental values (agreement better than ~0.05 Å) along all of the crystal axes. Generally, good agreement with X-ray diffraction data was also obtained for specific structural parameters, such as the interplanar porphyrin distance, mean deviation from planarity, Fe shift from the porphyrin plane, Fe–Fe and Fe–O bond lengths, etc. In contrast, uncorrected PBE exhibited markedly different behavior. Along the c axis, where the binding is predominantly due to hydrogen bonds between the free propionic acid groups of adjacent dimers, PBE yielded a lattice parameter in agreement with experiment. Indeed, PBE is well-known to provide a reasonable description of all but the weakest hydrogen bonds.[5] However, along the a axis, where the binding is mostly due to dispersive interactions between the methyl and vinyl side groups of adjacent dimers, PBE predicted a shallow minimum and significantly overestimated the lattice constant. Worse, along the b axis, where
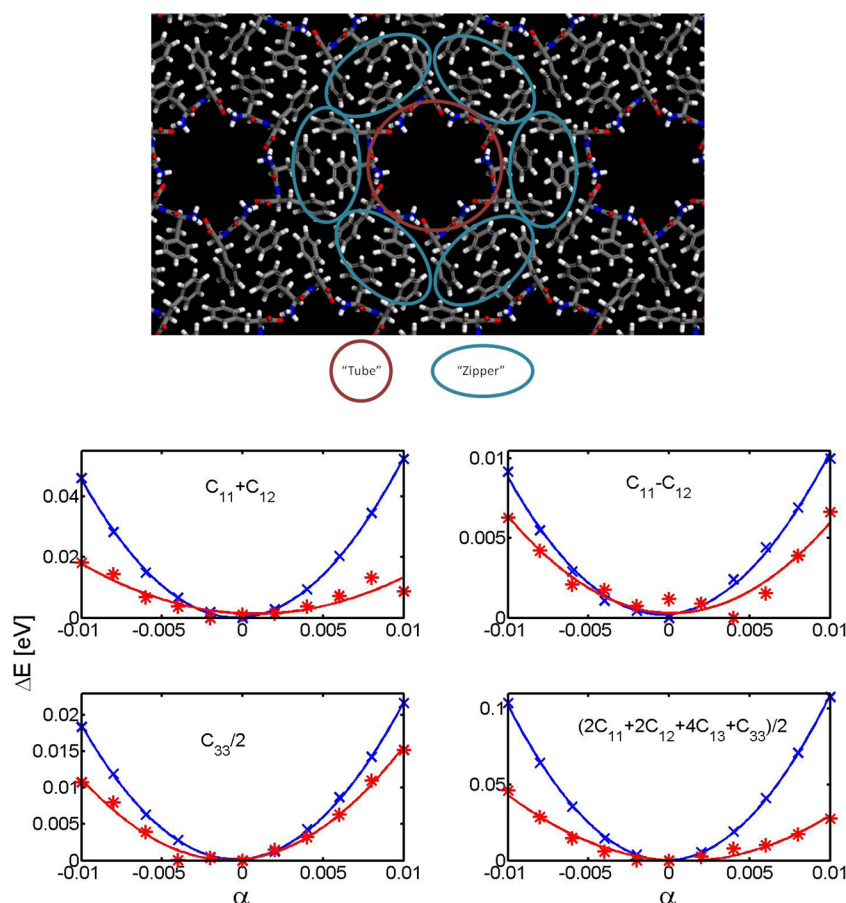
Figure 3. (top) Schematic partition of the diphenylalanine-based molecular solid into repeating building blocks consisting of an alanine-based "tube" surrounded by six "zipper" units consisting of two diphenyls each. (bottom) Plots of energy as a function of strain, computed with (blue crosses) and without (red asterisks) TS-vdW corrections, for the following distortions: equal expansion along the x and y axes (top left); equal expansion along the x axis and compression along the y axis (top right); expansion along the z axis (bottom left); and isotropic expansion (bottom right). Solid lines represent parabolic fits, and the elastic constant combination extracted from the curvature of each fit is denoted in each panel. Reproduced from ref 46. Copyright 2014 American Chemical Society.

the binding is predominantly due to $\pi-\pi$ interactions between the porphyrin rings of adjacent dimers, uncorrected PBE provided no minimum at all. Thus, properly accounting for dispersive interactions via pairwise corrections was found to possible and, furthermore, essential for describing the structure of synthetic hemozoin not only quantitatively but even qualitatively.[41]

The hemozoin crystal also demonstrates the practical importance of flexibility in the choice of the underlying xc functional[30] (as demonstrated in Figure 1 above) to obtain a satisfactory description of the electronic structure. While this has little effect on the geometry in this case, PBE is well-known to favor configurations with lower spin compared with hybrid functionals such as PBE0[44] (obtained from PBE by replacing 25% of the PBE exchange with Fock exchange). This tendency was also seen for the heme dimer, where PBE0+TS-vdW predicted the correct high-spin configuration with $J = 11$ while PBE + TS-vdW favored the $J = 7$ or $J = 5$ configuration.[41]

Beyond methodology confirmation, calculations of the relative stability of three stereoisomers as isolated dimers and in the unit cells of the two phases of hemozoin allowed for an explanation of the experimentally observed two distinct crystal phases, with somewhat different unit cells, as being associated with different stereoisomers. A growth mechanism wherein the first stage of nucleation is the formation of cyclic dimers was

suggested. In the ensuing crystallization stage, the centrosymmetric stereoisomer forms the major phase and the chiral noncentrosymmetric dimer, which is unlikely to adsorb on the growing faces of the major-phase crystal because of the stereochemical mismatch, segregates and forms the minor phase.[41]

A natural question, then, is whether the success obtained in structural prediction carries over to quantities related to second derivatives of the energy, such as elastic constants or vibrational properties. This has been demonstrated recently using several interesting test cases. The above-mentioned applications of TS-vdW to weakly bound solids[39,40] also indicate that they greatly improve the bulk modulus. In the context of the elastic response, an interesting and challenging system is diphenyla-lanine peptide, which self-assembles to form a bioinspired, supramolecular solid,[45] shown in Figure 3.[46] The nanotubular structures of this solid possess a variety of remarkable properties. In particular, they are unexpectedly stiff,[47,48] with reported Young's moduli of 19–27 GPa, which are much higher than one would naively assume for what is intuitively expected to be a soft material.

The chemical basis for this remarkable rigidity can be elucidated by first-principles calculations. Various combinations of elastic constants, allowing the extraction of Young's moduli, can be derived from the curvature of energy–strain curves

obtained by symmetry-guided distortions of the unit cell. Such energy—strain curves, shown in Figure 3,[46] yield two interesting observations. Qualitatively, energy—strain curves should ideally be parabolic within the elastic limit. The dispersion-corrected curves are visibly much more parabolic. This is the case because without dispersive attractions, some of the "glue" that keeps the structure together is gone, rendering the structure "less physical" and less chemically stable. In particular, the energy profile contains more than one energy minimum and is more shallow and corrugated. Quantitatively, the elastic constants are much larger with dispersive corrections. The obtained Young's modulus along the x direction, ∼9 GPa, is still smaller than the experimentally determined one, and some of this difference can ensue directly from our approximations. However, other explanations are plausible. First, simulations were performed on the bulk crystal, whereas all of the experiments were performed on a peptide tube. Second, the measured value was deduced from a finite-element analysis of the raw experimental data and is likely to be an overestimate. Third, trapping of residual water molecules inside the pores of the crystalline structure may affect the measured values. In view of these uncertainties, the value obtained in the calculations is sufficient to gain further insights.

Importantly, more than half of the Young's modulus in the x direction is attributed to dispersive interactions. This is a consequence of the unique supramolecular ordering in the crystal, illustrated in Figure 3,[46] in which the structural motif is partitioned into an array of peptide nanotube backbones with six interpenetrating "zipperlike" aromatic interlocks, each consisting of two diphenyls. Chemically, the interaromatic interaction is dominated by vdW forces. While each individual vdW interaction is relatively weak, there are many phenyl rings participating in the "zipperlike" structure, so the overall interaction is significant. The rigidity of the peptide backbone is expected to be highly influenced by interpeptide hydrogen bonding. Therefore, rigidity due to either type of bonding is increased by the inclusion of TS-vdW dispersive corrections. Detailed analysis of the stretching-induced relative displacements indicated the crucial role played by the "zipperlike" aromatic interlock in determining the rigidity. Specifically, the distortion associated with opening of the "cage structure" in the stretched direction was found to dominate over that associated with opening of the "zipper structure".

To demonstrate the accuracy of TS-vdW corrections for vibrational properties we consider brushite, CaHPO$_4$·2H$_2$O, a crystalline hydrated acidic form of calcium phosphate, shown in Figure 4a.[49] Brushite occurs in both physiological and pathological biomineralization processes.[50] Among calcium phosphates, brushite is particularly interesting because it possesses a double layer of water molecules that are intrinsically part of the lattice (Figure 4a). Therefore, while brushite is not, strictly speaking, a molecular crystal, it does contain molecular objects in the unit cell, and some aspects of its structure and properties are also sensitive to weak dispersive interactions.

As part of a comprehensive analysis of its infrared absorption spectrum[49] that generally resulted in quantitative agreement between theory and experiment, it was found that dispersive corrections play a particularly important role in the water libration modes, as shown in Figure 4b. Libration modes are rotational modes of the water molecule that are hindered by the rigid crystalline surroundings. For each crystallographic water unit, three normal modes of libration are expected. They are normally observed in a relatively broad spectral region.[52]
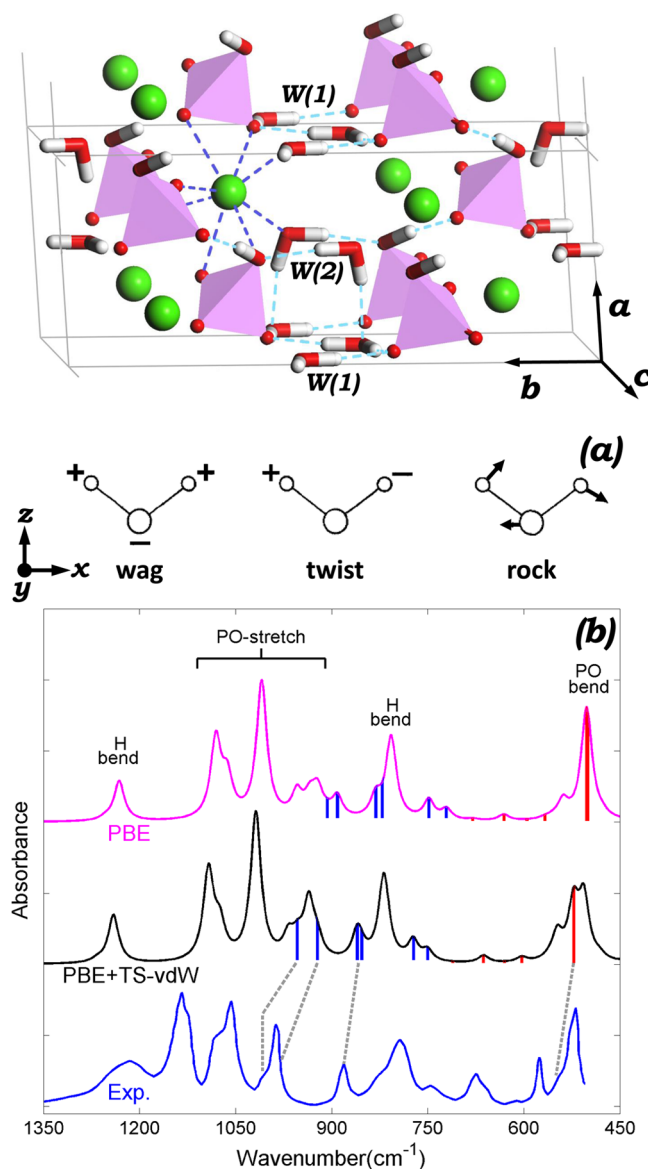

Figure 4. (a) Structure of brushite, containing Ca atoms (green), O atoms (red), H atoms (white), and phosphorus atoms, which are inside the purple tetrahedra representing the phosphate ions. For convenient visualization, more than a standard unit cell is shown. Standard unit cell vectors are depicted in the figure. (b) Three water libration modes and a comparison of the calculated (PBE and PBE+TS-vdW) and experimental[51] spectra at 77 K. Blue and red vertical lines represent libration mode frequencies corresponding to the W(1) and W(2) water molecules, respectively. Reproduced from ref 49. Copyright 2014 American Chemical Society.

Assignment of libration modes is often difficult even with deuteration and measurements at low temperature, as these modes span a large spectral region and overlap with other absorption features. In the theoretical spectrum, all of the libration modes were assigned. Figure 4b clearly indicates that the addition of the TS-vdW correction influences the energies of the libration modes, changing the overall shape of the spectrum and yielding better agreement with experiment. This is especially evident for bands marked by the gray dashed lines. These results are reasonable considering that the water libration is especially affected by vdW interactions between the water molecules and the rest of the crystalline environment. Thus,

libration modes calculated with vdW corrections improve our understanding of their contribution to the overall spectrum. We note in passing that beyond libration modes, these calculations allowed a definitive assignment of the debated stretching vibrations of the two types of water molecules in the unit cell.

With the above examples, we hope to have shown convincingly that significant progress in understanding the structure, stability, mechanical strength, and vibrational properties of molecular crystals has been made possible by employing TS-vdW pairwise additive descriptions of dispersion interactions in the context of DFT. However, it is well-known that the dispersion energy arises from collective electronic fluctuations in matter. Therefore, dispersion is a many-body phenomenon that demands a consistent quantum-mechanical description beyond simple pairwise models.[31,53] One option to go beyond those is to use quantum-chemical approaches or stochastic quantum Monte Carlo methods that aim toward the exact solution of the many-electron Schrödinger equation. These methods are potentially very accurate but in practice are very expensive because they require the solution of equations with large computational scaling powers and prefactors in terms of the number of electrons. To address the inherent many-body nature of long-range electron correlation energy, the Tkatchenko group has recently developed the so-called many-body dispersion (MBD) method.[54,55] It builds on the Tkatchenko–Scheffler approach described above by using the TS projection of the many-electron system into an auxiliary set of quantum harmonic oscillators (QHOs).[27] This model system of QHOs is parametrized "on-the-fly" to reproduce the dipole response properties of the real electronic system using only its electron density. This parametrization works successfully for both molecules and solids with a finite electronic gap, reproducing their polarizabilities and C_6 coefficients with an accuracy of 5−7%.

Furthermore, an analytical proof demonstrating the equivalence between the MBD energy expression and the correlation energy in the random-phase approximation (RPA) for a system of dipolar QHOs has been given.[31] In contrast to RPA calculations based on DFT orbitals, MBD avoids explicit use of single-electron orbitals, allowing for a negligible computational cost with respect to a self-consistent DFT calculation. The MBD method[54,55] has proven to be very accurate for a variety of molecular and solid-state systems, consistently achieving accuracies of 5−7% with respect to high-level reference binding energies for (supra)molecular systems[54−57] and lattice energies of molecular crystals.[56,58−61] The accuracy of DFT+MBD calculations is in fact often within the uncertainty of the reference data.[57,60]

Figure 5 compares the performance of the MBD and TS-vdW schemes for the S66 molecular complex set,[37] the S12L benchmark set of larger, more complex intermolecular interactions,[62] and the X23 database of experimental molecular-crystal lattice energies.[60,61] Clearly, MBD offers improvement for all three sets, but the improvement is much more pronounced for the larger complexes and the molecular solids, indicating the important role of beyond-pairwise interactions in such systems.

To better understand the emergence of nontrivial many-body effects in coupled QHO systems, it is useful to distinguish between two classes of contributions. Dispersion energies can be computed as spatial integrals over a frequency-dependent polarizability, which is by definition a nonadditive tensor that depends in a highly nonlinear fashion on the fluctuating electric
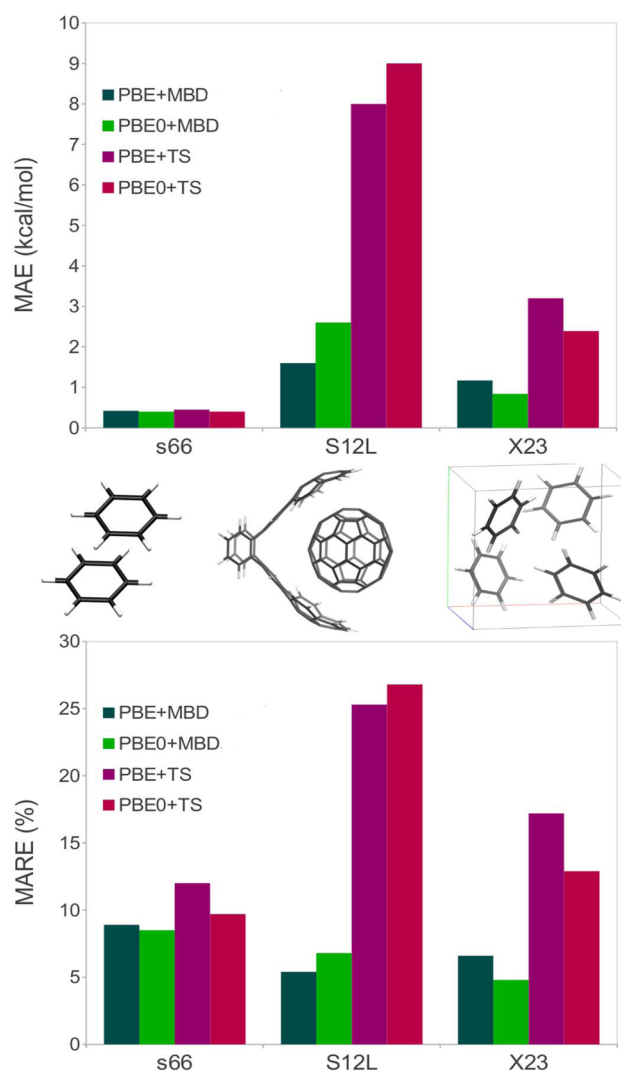

Figure 5. (top) Mean absolute errors (MAEs, in kcal/mol) and (bottom) mean absolute relative errors (MAREs, in %) for the S66, S12L, and X23 databases computed with the TS and MBD methods combined with both the PBE and PBE0 functionals. The middle panel shows a representative complex from each of the three databases: (left) benzene dimer, (center) "buckycatcher" ($C_{60}@C_{60}H_{28}$), and (right) benzene crystal. Reproduced with permission from ref 55. Copyright 2014 American Institute of Physics.

fields inside molecules and materials. The polarizability relates induced dipole moments to applied electric fields, and since both quantities are vectorial, the polarizability is usually an anisotropic tensor. In the context of empirical dispersion corrections, the polarizability is often crudely approximated as a scalar that depends only on the local hybridization environment, for example having slightly different (on the order of 10−15%) isotropic values for sp-, sp^2-, and sp^3-hybridized carbons. However, this ignores the sensitive dependence of polarizability on ever-present internal electric fields, which can lead to dramatic modifications. This was illustrated recently by carbon nanostructures of different size and dimensionality.[63] It was found that the C_6 coefficient per carbon atom varies from around 20 hartree·bohr^6 in diamond to 147 hartree·bohr^6 in graphene, with other carbon nanostructures showing intermediate values. These large modifications categorically demonstrate the importance of the anisotropic response in

low-dimensional nanostructures, where dipoles align along certain preferred directions (e.g., in the plane of graphene or along the long axis of a nanotube). Indeed, many-body effects in the polarizability have been shown to dramatically affect the interlayer binding energy of graphite, even leading to self-assembly behavior that is qualitatively different than that predicted by simple pairwise models. For example, it has been suggested that the binding energy of fullerene on a multilayered graphene stack *decreases* as a function of the number of graphene layers, whereas a pairwise theory yields an *increasing* binding energy.[63] We stress that electrodynamic polarization effects are abundant even in small molecules. For example, the polarizability of the nitrogen dimer is anisotropic, with experimental values of $\alpha_{xx,yy} = 9.8$ bohr^3 and $\alpha_{zz} = 16.1$ bohr^3, where z is the molecular axis.[64]

A different type of many-body effect involves the well-known many-body energy terms, such as the Axilrod−Teller−Muto (ATM) interaction between three closed-shell atoms.[65] In contrast to pairwise energies, which are always attractive, the ATM energy can be attractive or repulsive depending on the angles in the triangle formed by the three atoms.[66] The importance of many-body terms in the dispersion energy has recently been assessed by several different groups.[26,62,66−68] It was found that these terms should be included for an accurate description of binding energies in large molecular assemblies. Beyond the ATM term, there are N-body interactions, where N is the number of particles (electrons, atoms, or molecules). Several groups have recently demonstrated that ATM terms often do not dominate beyond the pairwise energy, and higher-order terms can play an important role in achieving "chemical accuracy". A many-body decomposition analysis of the dispersion energy clearly demonstrated that energy contributions up to six-body interactions are required in order to achieve an accuracy of 1 kcal/mol in the binding of supramolecular systems.[57] For larger, more polarizable materials such as nanotubes, the dispersion energy has to be computed up to *infinite order*, as any low-order truncation of the energy leads to significant deviations in the computed binding energy of a double-walled carbon nanotube.[57]

Compared with other organic materials, molecular crystals exhibit especially interesting many-body effects. In particular, molecular packing into multiple crystal forms (polymorphs) leads to polymorph-dependent polarization behavior, and in this case the subtle interplay between many-body terms dictates the relative stability of different polymorphs. In some cases, the pairwise dispersion energy is sufficient for a correct identification of relative polymorph stability.[69,70] However, only upon inclusion of many-body effects could one account for the experimentally derived relative stabilities of the α, β, and γ polymorphs of the glycine crystal.[59] Similar conclusions were obtained for the relative stabilities of polymorphs of oxalic and tetrolic acids.[59] For oxalic acid, widely used pairwise corrections overstabilize the α form, while the two forms should be essentially degenerate according to experiment. These findings demonstrate that including MBD effects in DFT can lead to qualitative changes in the relative stabilities of polymorphic molecular crystals compared with pairwise dispersion corrections. Clearly, significantly more work is required in order to understand which systems are the ones where MBD effects are particularly strong and lead to the emergence of novel behavior that cannot be described by simple pairwise methods. The development of MBD methods is an active research field, and

we expect to see further developments and understanding of many-body effects in the dispersion energy in the near future.

Despite the fact that dispersion-inclusive density functionals have enjoyed considerable attention and have been rather successfully applied to a wide variety of materials, there is clearly room for further improvement. One particular issue is the infamous delocalization or self-interaction error, which is present in all semilocal and conventional hybrid DFT functionals. Because hybrid functionals mitigate these errors, one would expect hybrid functionals typically to perform better than pure semilocal generalized gradient approximation (GGA) functionals. This is often the case, as shown in Figures 1 and 5. However, Figure 5 also shows that for supramolecular complexes the hybrid PBE0 functional coupled with the MBD method yields larger errors than the parent semilocal PBE functional. This may indicate that more advanced range-separated hybrid (RSH) functionals[71,72] could assist in capturing the subtle non-covalent interactions in systems with strong inhomogeneous polarization. Indeed, coupling RSH functionals with MBD leads to improved performance for small molecular dimers in the S66 database.[36]

In conclusion, we have provided an overview of some important cases where the simple, minimally empirical pairwise correction scheme of Tkatchenko and Scheffler provides a useful prediction of structures and response properties. We have further shown that this scheme is not always sufficiently accurate. In such cases, it can be augmented by a computationally inexpensive many-body dispersion approach that often results in useful quantitative accuracy even in the presence of significant screening and/or multibody contributions to the dispersive energy. Throughout, we have illustrated this using a selection of biological or bioinspired molecular crystals with an emphasis on lessons learned not only for the methodology but also for the chemistry and physics of the crystals in question.

■ AUTHOR INFORMATION

Corresponding Authors

*E-mail: leeor.kronik@weizmann.ac.il.
*E-mail: tkatchen@fhi-berlin.mpg.de.

Notes

Biographies

Leeor Kronik obtained his Ph.D. in Physical Electronics in 1996 at Tel Aviv University. Presently he chairs the Department of Materials and Interfaces at the Weizmann Institute of Science, where he leads a group devoted to the quantum theory of real materials. He is a Fellow of the American Physical Society and a Member of the Israeli Young National Academy and has received the Young Scientist Award of the Israel Chemical Society (2010) and the Young Scientist Krill Prize of the Wolf Foundation (2006).

Alexandre Tkatchenko obtained his Ph.D. in Physical Chemistry in 2007 at the Universidad Autonoma Metropolitana, Mexico. During 2008−2010 he was an Alexander von Humboldt Fellow in the Theory Department at FHI, Berlin. Currently, he leads the Functional Materials and Intermolecular Interactions Group at FHI. He has received the Gerhard Ertl Young Investigator Award of the German Physical Society (2011).

■ REFERENCES

(1) Wright, J. D. *Molecular Crystals*, 2nd ed.; Cambridge University Press: Cambridge, U.K., 1995.

(2) Dreizler, R. M.; Gross, E. K. U. *Density Functional Theory*; Springer: Berlin, 1990.

(3) Parr, R. G.; Yang, W. *Density Functional Theory of Atoms and Molecules*; Oxford University Press: Oxford, U.K., 1989.

(4) *A Primer in Density Functional Theory*; Fiolhais, C., Nogueira, F., Marques, M. A., Eds.; Lecture Notes in Physics, Vol. *620*; Springer: Berlin, 2003.

(5) Koch, W.; Holthausen, M. C. *A Chemist's Guide to Density Functional Theory*; Wiley-VCH: Weinheim, Germany, 2001.

(6) Martin, R. M. *Electronic Structure: Basic Theory and Practical Methods*; Cambridge University Press: Cambridge, U.K., 2004.

(7) Sholl, D. S.; Steckel, J. A. *Density Functional Theory: A Practical Introduction*; Wiley-Interscience: New York, 2009.

(8) Klimeš, J.; Michaelides, A. Perspective: Advances and challenges in treating van der Waals dispersion forces in density functional theory. *J. Chem. Phys.* **2012**, *137*, No. 120901.

(9) Riley, K. E.; Pitoňák, M.; Jurečka, P.; Hobza, P. Stabilization and Structure Calculations for Noncovalent Interactions in Extended Molecular Systems Based on Wave Function and Density Functional Theories. *Chem. Rev.* **2010**, *110*, 5023–5063.

(10) Langreth, D. C.; Lundqvist, B. I.; Chakarova-Käck, S. D.; Cooper, V. R.; Dion, M.; Hyldgaard, P.; Kelkkanen, A.; Kleis, J.; Kong, L.; Li, S.; Moses, P. G.; Murray, E.; Puzder, A.; Rydberg, H.; Schröder, E.; Thonhauser, T. A Density Functional for Sparse Matter. *J. Phys.: Condens. Matter* **2009**, *21*, No. 084203.

(11) Byrd, E. F. C.; Scuseria, G. E.; Chabalowski, C. F. An ab Initio Study of Solid Nitromethane, HMX, RDX, and CL20: Successes and Failures of DFT. *J. Phys. Chem. B* **2004**, *108*, 13100–13106.

(12) Tkatchenko, A.; Romaner, L.; Hofmann, O. T.; Zojer, E.; Ambrosch-Draxl, C.; Scheffler, M. Van der Waals Interactions between Organic Adsorbates and at Organic/Inorganic Interfaces. *MRS Bull.* **2010**, *35*, 435–442.

(13) Goerigk, L. How Do DFT-DCP, DFT-NL, and DFT-D3 Compare for the Description of London-Dispersion Effects in Conformers and General Thermochemistry? *J. Chem. Theory Comput.* **2014**, *10*, 968–980.

(14) Paier, J.; Ren, X.; Rinke, P.; Scuseria, G. E.; Gruneis, A.; Kresse, G.; Scheffler, M. Assessment of correlation energies based on the random-phase approximation. *New J. Phys.* **2012**, *14*, No. 043002.

(15) Xu, X.; Goddard, W. A., III. The X3LYP extended density functional for accurate descriptions of nonbond interactions, spin states, and thermochemical properties. *Proc. Natl. Acad. Sci. U.S.A.* **2004**, *101*, 2673–2677.

(16) Zhao, Y.; Truhlar, D. G. Density Functionals with Broad Applicability in Chemistry. *Acc. Chem. Res.* **2008**, *41*, 157–167.

(17) Peverati, R.; Truhlar, D. G. An improved and broadly accurate local approximation to the exchange–correlation density functional: The MN12-L functional for electronic structure calculations in chemistry and physics. *Phys. Chem. Chem. Phys.* **2012**, *14*, 13171–13174.

(18) Grimme, S. Semiempirical hybrid density functional with perturbative second-order correlation. *J. Chem. Phys.* **2006**, *124*, No. 034108.

(19) Kozuch, S.; Martin, J. M. L. DSD-PBEP86: In search of the best double-hybrid DFT with spin-component scaled MP2 and dispersion corrections. *Phys. Chem. Chem. Phys.* **2011**, *13*, 20104–20107.

(20) von Lilienfeld, O. A.; Tavernelli, I.; Röthlisberger, U.; Sebastiani, D. Optimization of Effective Atom Centered Potentials for London Dispersion Forces in Density Functional Theory. *Phys. Rev. Lett.* **2004**, *93*, No. 153004.

(21) Torres, E.; DiLabio, G. A. A (Nearly) Universally Applicable Method for Modeling Noncovalent Interactions Using B3LYP. *J. Phys. Chem. Lett.* **2012**, *3*, 1738–1744.

(22) Karalti, O.; Su, X.; Al-Saidi, W. A.; Jordan, K. D. Correcting density functionals for dispersion interactions using pseudopotentials. *Chem. Phys. Lett.* **2014**, *591*, 133–136.

(23) Gianturco, F. A.; Paesani, F. In *Conceptual Perspectives in Quantum Chemistry*; Calais, J. L., Kryachko, E., Eds.; Kluwer Academic Publishers: Dordrecht, The Netherlands, 1997; pp 337–382.

(24) Johnson, E. R.; Becke, A. D. A post-Hartree–Fock model of intermolecular interactions: Inclusion of higher-order corrections. *J. Chem. Phys.* **2006**, *124*, No. 174104.

(25) Grimme, S. Semiempirical GGA-type density functional constructed with a long-range dispersion correction. *J. Comput. Chem.* **2006**, *27*, 1787–1799.

(26) Grimme, S.; Antony, J.; Ehrlich, S.; Krieg, H. A consistent and accurate ab initio parametrization of density functional dispersion correction (DFT-D) for the 94 elements H–Pu. *J. Chem. Phys.* **2010**, *132*, No. 154104.

(27) Tkatchenko, A.; Scheffler, M. Accurate Molecular van der Waals Interactions from Ground-State Electron Density and Free-Atom Reference Data. *Phys. Rev. Lett.* **2009**, *102*, No. 073005.

(28) Corminboeuf, C. Minimizing Density Functional Failures for Non-Covalent Interactions Beyond van der Waals Complexes. *Acc. Chem. Res.* **2014**, DOI: 10.1021/ar400303a.

(29) van de Streek, J.; Neumann, M. A. Validation of experimental molecular crystal structures with dispersion-corrected density functional theory calculations. *Acta Crystallogr.* **2010**, *B66*, 544–558.

(30) Marom, N.; Tkatchenko, A.; Scheffler, M.; Kronik, L. Describing Both Dispersion Interactions and Electronic Structure Using Density Functional Theory: The Case of Metal–Phthalocyanine Dimers. *J. Chem. Theory Comput.* **2010**, *6*, 81–90.

(31) Tkatchenko, A.; Ambrosetti, A.; DiStasio, R. A., Jr. Interatomic methods for the dispersion energy derived from the adiabatic connection fluctuation–dissipation theorem. *J. Chem. Phys.* **2013**, *138*, No. 074106.

(32) Hirshfeld, F. L. Bonded-Atom Fragments for Desribing Molecular Charge Densities. *Theor. Chim. Acta* **1977**, *44*, 129–138.

(33) Bučko, T.; Lebègue, S.; Hafner, J.; Ángyán, J. G. Improved Density Dependent Correction for the Description of London Dispersion Forces. *J. Chem. Theory Comput.* **2013**, *9*, 4293–4299.

(34) Jurečka, P.; Šponer, J.; Černý, J.; Hobza, P. Benchmark database of accurate (MP2 and CCSD(T) complete basis set limit) interaction energies of small model complexes, DNA base pairs, and amino acid pairs. *Phys. Chem. Chem. Phys.* **2006**, *8*, 1985–1993.

(35) Marom, N.; Tkatchenko, A.; Rossi, M.; Gobre, V. V.; Hod, O.; Scheffler, M.; Kronik, L. Dispersion Interactions with Density-Functional Theory: Benchmarking Semiempirical and Interatomic Pairwise Corrected Density Functionals. *J. Chem. Theory Comput.* **2011**, *7*, 3944–3951.

(36) Agrawal, P.; Tkatchenko, A.; Kronik, L. Pair-Wise and Many-Body Dispersive Interactions Coupled to an Optimally Tuned Range-Separated Hybrid Functional. *J. Chem. Theory Comput.* **2013**, *9*, 3473–3478.

(37) Řezáč, J.; Riley, K. E.; Hobza, P. S66: A well-balanced database of benchmark interaction energies relevant to biomolecular structures. *J. Chem. Theory Comput.* **2011**, *7*, 2427–2438.

(38) Takatani, T.; Hohenstein, E. G.; Malagoli, M.; Marshall, M. S.; Sherrill, C. D. Basis set consistent revision of the S22 test set of noncovalent interaction energies. *J. Chem. Phys.* **2010**, *132*, No. 144104.

(39) Al-Saidi, W. A.; Voora, V. K.; Jordan, K. D. An Assessment of the vdW-TS Method for Extended Systems. *J. Chem. Theory Comput.* **2012**, *8*, 1503–1513.

(40) Bučko, T.; Lebègue, S.; Hafner, J.; Ángyán, J. G. Tkatchenko–Scheffler van der Waals correction method with and without self-

consistent screening applied to solids. *Phys. Rev. B* **2013**, *87*, No. 064110.

(41) Marom, N.; Tkatchenko, A.; Kapishnikov, S.; Kronik, L.; Leiserowitz, L. Structure and Formation of Synthetic Hemozoin: Insights from First-Principles Calculations. *Cryst. Growth Des.* **2011**, *11*, 3332–3341.

(42) Fong, K. Y.; Wright, D. W. Hemozoin and antimalarial drug discovery. *Future Med. Chem.* **2013**, *5*, 1437–1450.

(43) Perdew, J. P.; Burke, K.; Ernzerhof, M. Generalized Gradient Approximation Made Simple. *Phys. Rev. Lett.* **1996**, *77*, 3865–3868.

(44) Perdew, J. P.; Ernzerhof, M.; Burke, K. Rationale for mixing exact exchange with density functional approximations. *J. Chem. Phys.* **1996**, *105*, 9982–9985.

(45) Reches, M.; Gazit, E. Casting Metal Nanowires within Discrete Self-Assembled Peptide Nanotubes. *Science* **2003**, *300*, 625–627.

(46) Azuri, I.; Adler-Abramovich, L.; Gazit, E.; Hod, O.; Kronik, L. Why Are Diphenylalanine-Based Peptide Nanostructures So Rigid? Insights from First Principles Calculations. *J. Am. Chem. Soc.* **2014**, *136*, 963–969.

(47) Kol, N.; Adler-Abramovich, L.; Barlam, D.; Shneck, R. Z.; Gazit, E.; Rousso, I. Self-assembled peptide nanotubes are uniquely rigid bioinspired supramolecular structures. *Nano Lett.* **2005**, *5*, 1343–1346.

(48) Niu, L.; Chen, X.; Allen, S.; Tendler, S. J. Using the bending beam model to estimate the elasticity of diphenylalanine nanotubes. *Langmuir* **2007**, *23*, 7443–7446.

(49) Hirsch, A.; Azuri, I.; Addadi, L.; Weiner, S.; Yang, K.; Curtarolo, S.; Kronik, L. Infrared Absorption Spectrum of Brushite from First Principles. *Chem. Mater.* **2014**, *26*, 2934–2942.

(50) LeGeros, R. Z.; Legeros, J. P. In *Phosphate Minerals*; Nriagu, J. O., Moore, P. B., Eds.; Springer: Berlin, 1984; pp 351–385.

(51) Trpkovska, M.; Šoptrajanov, B.; Malkov, P. FTIR reinvestigation of the spectra of synthetic brushite and its partially deuterated analogues. *J. Mol. Struct.* **1999**, *480*, 661–666.

(52) Lutz, H. D. *Solid Materials*; Springer: Berlin, 1988; pp 97–125.

(53) Dobson, J. F. Beyond pairwise additivity in London dispersion interactions. *Int. J. Quantum Chem.* **2014**, DOI: 10.1002/qua.24635.

(54) Tkatchenko, A.; DiStasio, R. A., Jr.; Car, R.; Scheffler, M. Accurate and Efficient Method for Many-Body van der Waals Interactions. *Phys. Rev. Lett.* **2012**, *108*, No. 236402.

(55) Ambrosetti, A.; Reilly, A. M.; DiStasio, R. A., Jr.; Tkatchenko, A. Long-range correlation energy calculated from coupled atomic response functions. *J. Chem. Phys.* **2014**, *140*, No. 18A508.

(56) DiStasio, R. A., Jr.; von Lilienfeld, O. A.; Tkatchenko, A. Collective many-body van der Waals interactions in molecular systems. *Proc. Natl. Acad. Sci. U.S.A.* **2012**, *109*, 14791–14795.

(57) Ambrosetti, A.; Alfe, D.; DiStasio, R. A., Jr.; Tkatchenko, A. Hard Numbers for Large Molecules: Toward Exact Energetics for Supramolecular Systems. *J. Phys. Chem. Lett.* **2014**, *5*, 849–855.

(58) Schatschneider, B.; Liang, J. J.; Reilly, A. M.; Marom, N.; Zhang, G. X.; Tkatchenko, A. Electrodynamic response and stability of molecular crystals. *Phys. Rev. B* **2013**, *87*, No. 060104(R).

(59) Marom, N.; DiStasio, R. A., Jr.; Atalla, V.; Levchenko, S.; Reilly, A. M.; Chelikowsky, J. R.; Leiserowitz, L.; Tkatchenko, A. Many-Body Dispersion Interactions in Molecular Crystal Polymorphism. *Angew. Chem., Int. Ed.* **2013**, *52*, 6629–6632.

(60) Reilly, A. M.; Tkatchenko, A. Seamless and Accurate Modeling of Organic Molecular Materials. *J. Phys. Chem. Lett.* **2013**, *4*, 1028–1033.

(61) Reilly, A. M.; Tkatchenko, A. Understanding the role of vibrations, exact exchange, and many-body van der Waals interactions in the cohesive properties of molecular crystals. *J. Chem. Phys.* **2013**, *139*, No. 024705.

(62) Risthaus, T.; Grimme, S. Benchmarking of London dispersion-accounting density functional theory methods on very large molecular complexes. *J. Chem. Theory Comput.* **2013**, *9*, 1580–1591.

(63) Gobre, V. V.; Tkatchenko, A. Scaling laws for van der Waals interactions in nanostructured materials. *Nat. Commun.* **2013**, *4*, No. 2341.

(64) Thole, B. T. Molecular polarizabilities calculated with a modified dipole interaction. *Chem. Phys.* **1981**, *59*, 341–350.

(65) Axilrod, B. M.; Teller, E. Interaction of the van der Waals type between three atoms. *J. Chem. Phys.* **1943**, *11*, 299–300.

(66) von Lilienfeld, O. A.; Tkatchenko, A. Two- and three-body interatomic dispersion energy contributions to binding in molecules and solids. *J. Chem. Phys.* **2010**, *132*, No. 234109.

(67) Otero-de-la Roza, A.; Johnson, E. R. Many-body dispersion interactions from the exchange-hole dipole moment model. *J. Chem. Phys.* **2013**, *138*, No. 054103.

(68) Silvestrelli, P. L. Van der Waals interactions in density functional theory by combining the quantum harmonic oscillator-model with localized Wannier functions. *J. Chem. Phys.* **2013**, *139*, No. 054106.

(69) Pedone, A.; Presti, D.; Menziani, M. C. On the ability of periodic dispersion-corrected DFT calculations to predict molecular crystal polymorphism in *para*-diiodobenzene. *Chem. Phys. Lett.* **2012**, *541*, 12–15.

(70) Santra, B.; Klimeš, J.; Alfè, D.; Tkatchenko, A.; Slater, B.; Michaelides, A.; Car, R.; Scheffler, M. Hydrogen Bonds and van der Waals Forces in Ice at Ambient and High Pressures. *Phys. Rev. Lett.* **2011**, *107*, No. 185701.

(71) Kronik, L.; Stein, T.; Refaely-Abramson, S.; Baer, R. Excitation Gaps of Finite-Sized Systems from Optimally Tuned Range-Separated Hybrid Functionals. *J. Chem. Theory Comput.* **2012**, *8*, 1515–1531.

(72) Refaely-Abramson, S.; Sharifzadeh, S.; Jain, M.; Baer, R.; Neaton, J. B.; Kronik, L. Gap renormalization of molecular crystals from density-functional theory. *Phys. Rev. B* **2013**, *88*, No. 081204(R).